WEP Warwick Evans Publishing

International Journal of Natural Resources and Environmental Studies

ISSN: 3006-2012 (Print), ISSN: 3006-0834 (Online) | Volume 8, Number 4, Year 2026
DOI: https://doi.org/10.62051/ijnres.v8n4.08
Journal homepage: https://wepub.org/index.php/IJNRES/index

Study on Summer Thermal Comfort and Its Influencing Factors in the Qingshan Lake Greenway

Yining Yao[1], Wenhui Xu[*]

[1]College of Landscape and Architecture, Zhejiang A&F University, Hangzhou 311300, China
*Corresponding Author: Wenhui Xu

ABSTRACT

As urbanization accelerates, the urban heat island (UHI) effect increasingly impacts the ecological environment and residents' thermal comfort. Greenways, functioning as multifunctional linear green open spaces, play a vital role in improving the urban thermal environment. However, the mechanisms by which internal spatial characteristics affect microclimate and thermal comfort remain unclear. Taking 10 spatial types within the Qingshan Lake Greenway as a case study, this research utilized measured microclimatic data to calculate the Physiological Equivalent Temperature (PET), revealing the spatiotemporal variations of thermal comfort within the greenway. Concurrently, an indicator system for greenway spatial characteristics was established. Correlation analysis and stepwise regression models were applied to uncover the impact mechanisms of various spatial features on the microclimate and thermal comfort. The results indicate that: (1) Within the Qingshan Lake Greenway, the degree of shading exerts a more substantial influence on human thermal comfort than water body area. The comprehensive thermal comfort across different periods ranked as follows: 17:30–18:30 > 09:30–10:30 > 16:30–17:30 > 10:30–11:30. (2) Greenway spatial characteristics significantly influence air temperature, relative humidity, and globe temperature, whereas the effects on wind speed and solar radiation are comparatively minor. (3) The green space ratio, green view index (GVI), permeable surface ratio, spatial coverage, spatial enclosure, and sky view factor (SVF) significantly affect human thermal comfort. The stepwise regression equation linking average PET to these influencing factors is expressed as: PETmean = 40.261 + 1.157 * green space ratio – 1.331 * subsurface permeability rate – 5.390 * coverage degree. These findings provide crucial guidance for optimizing the internal spaces of suburban greenways and enhancing the thermal comfort of human settlements.

KEYWORDS

Greenway; Microclimate; Thermal comfort; Spatial characteristics; Physiological Equivalent Temperature (PET).

1. INTRODUCTION

With the continuous advancement of urbanization, the surge in anthropogenic heat generated by vehicles and industries [1] has intensified the urban heat island (UHI) effect [2], posing severe threats to the ecological environment, public health, and residents' thermal comfort [3]. Studies have shown that improving the local urban microclimate can effectively alleviate thermal stress [4],[5], playing a positive role in enhancing the urban environment and promoting sustainable urban development. Currently, extensive microclimatic research has been conducted on various outdoor public spaces, including urban parks [6], residential areas [7], and university campuses [8].

As multifunctional linear green open spaces connecting biological habitats, natural landscape elements, and urban communities, greenways possess crucial ecological value. They not only prevent

soil erosion, purify water sources, and improve air quality but also mitigate the UHI effect during summer, providing high-quality recreational spaces for residents and thereby enhancing their overall quality of life. The microclimate of greenway spaces has gradually garnered increasing attention. Related studies typically employ three primary methods to evaluate the thermal environment of greenways: remote sensing technology, field observations, and numerical simulations. For instance, Liang evaluated the thermal comfort of the Donghaochong and Liwanchong greenways by investigating users' thermal sensations and comfort levels through questionnaires, identifying temperature as the critical determinant of thermal sensation and comfort [9]. Similarly, taking the "Three Hills and Five Gardens" greenway in Beijing as a case study, Li collected field measurement data to analyze the greenway microclimate from four perspectives: plant community composition, planting density, community diversity, and paving materials. Furthermore, the correlation between environmental parameters (e.g., temperature, humidity, and wind speed) and the thermal comfort indices (PMV-PPD) was explored [10].

Current research on greenway thermal environments primarily focuses on their cooling effects, the spatiotemporal distribution characteristics of temperature and humidity, and the impact of greenway design elements on microclimates. Moreover, most studies concentrate on the macro-scale thermal environment. There remains a notable lack of research regarding the relationship between the internal spatial characteristics of greenways, microclimate, and thermal comfort. In particular, the underlying correlation mechanisms between micro-scale internal spatial characteristics and thermal comfort have not been fully elucidated. Therefore, it is essential to clarify the varying capacities of different greenway spatial characteristics in improving microclimate and thermal comfort, and to explore the correlational mechanisms between them.

In light of this, taking the Qingshan Lake Greenway as a case study, the primary objectives of this research are to: (1) conduct field measurements of air temperature, relative humidity, wind speed, solar radiation, and globe temperature across different time periods and spatial types within the greenway, and calculate the PET for each spatial type at various times; (2) establish an indicator system for greenway spatial characteristics and, based on unmanned aerial vehicle (UAV) imagery and ground surveys, utilize semantic segmentation to extract and analyze relevant indices of the sample plots, such as the green view index (GVI), blue view index (BVI), hardscape view index, and spatial coverage; (3) apply stepwise regression analysis to reveal the relationships between these indices and thermal comfort. This study aims to provide guiding recommendations for the internal spatial optimization and thermal comfort enhancement of suburban greenways.

2. MATERIALS AND METHODS

2.1. Study Area

Lin'an District is located in the northwest of Hangzhou City, Zhejiang Province, China (29°56′–30°23′ N, 118°51′–119°52′ E), and features a subtropical monsoon climate. The annual average precipitation is approximately 1500–1800 mm, and the annual average temperature is about 16–17 °C. The hottest months are July and August, with an average maximum temperature of around 30–33 °C, exhibiting typical characteristics of hot summers and cold winters. This study selected the Qingshan Lake Greenway in Lin'an District (30°13′–30°16′ N, 119°45′–119°48′ E) as the research area (Figure 1). The selection of this site was based on three primary reasons:

(1) The Qingshan Lake Greenway boasts a rich hierarchy of plant species and encompasses a comprehensive and diverse range of landscape elements and spatial types. Its representativeness and uniqueness enable it to comprehensively reflect the actual climatic conditions of suburban greenways in Hangzhou.

(2) Situated at the western end of the Hangzhou Chengxi Sci-Tech Innovation Corridor, the greenway enjoys convenient transportation and high accessibility. With abundant natural resources and profound historical and cultural heritage, it performs essential urban service functions, thus preventing potential biases in the research results caused by unfavorable geographical locations [11].

(3) As an ideal destination for Hangzhou residents and surrounding tourists to connect with nature, exercise, and relax, the greenway experiences dense human activity and holds considerable regional influence. Consequently, investigating its internal microclimatic characteristics and thermal comfort bears strong practical significance and regional application value.

Built along the Qingshan Lake Reservoir, the Qingshan Lake Greenway has a lake-frontage rate of 80% and a total length of 42.195 km. Based on its functions and current resource characteristics, it is planned and designed into six landscape sections with distinct styles, forming an overall spatial layout of "one center, three nodes, and six sections." Since one section of the greenway is still under planning, the five completed and operational main routes were selected as the specific research objects.

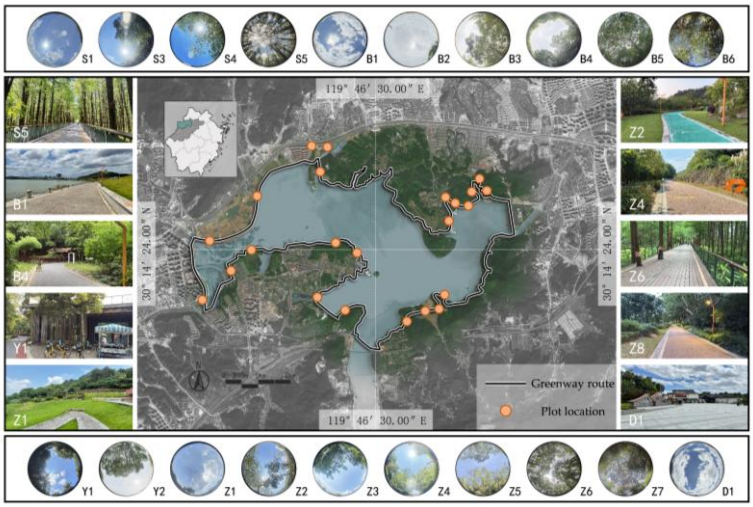

Figure 1. Study area and sample site selection.

Prior to the selection of sample sites, a comprehensive field survey of the entire greenway was conducted to document its spatial types. Subsequently, the degree of overhead shading and the distance to the water surface were adopted as classification criteria. The degree of shading was categorized based on the sky view factor (SVF) [12]. SVF values were obtained by capturing vertical sky photographs with a fisheye lens, followed by grayscale processing and proportion calculation using Photoshop. Specifically, an SVF < 0.1 was defined as fully shaded, 0.45 < SVF < 0.55 as semi-shaded, and SVF > 0.95 as unshaded (open).

Based on these spatial classification criteria, at least two representative sample sites were selected for each type. Ultimately, 10 types of greenway spaces were identified: open water area, semi-shaded water area, fully shaded water area, open waterfront area, semi-shaded waterfront area, fully shaded waterfront area, semi-shaded hardscape area, open lawn area, semi-shaded understory area, and fully shaded understory area. In addition, an unshaded hardscape open space at the greenway entrance was designated as the control site, yielding a total of 23 sample sites. These sites are distributed across all sections of the greenway. Because variations in microclimate and improvements in human thermal comfort are more pronounced in areas located 10–20 m from the water body [13], the waterfront measurement points were all situated within 20 m of the lake surface. Previous studies have indicated that the minimum effective distance of landscape influence on microclimate is 10 m [14],[15]. Considering the actual spatial dimensions of the Qingshan Lake Greenway, the size of each sample plot was standardized to 20 m × 20 m.

2.2. Indicator Selection

2.2.1. Selection of Thermal Comfort Evaluation Indices

Thermal comfort generally refers to the perceived state of comfort of an individual within a specific localized space. Its evaluation methods include objective calculations based on physical models and subjective perception analyses based on questionnaire surveys. Commonly used physical model indices for objective calculation include Predicted Mean Vote (PMV), Physiological Equivalent Temperature (PET), Standard Effective Temperature (SET*), and Universal Thermal Climate Index (UTCI) [16]. Meanwhile, subjective thermal perception indices primarily include Thermal Sensation Vote (TSV) and Thermal Comfort Vote (TCV). In this study, the PET model was selected as the evaluation index for human thermal comfort, and RayMan Pro software was utilized to calculate the PET values for the following reasons:

(1) The PET model in the RayMan Pro software can comprehensively integrate multiple influencing factors, including geographical location, local climatic parameters, measurement time points, individual physiological characteristics, activity intensity, and clothing insulation [17]. Because of its ability to coordinate and synthesize these diverse elements, PET is considered a scientifically robust and reasonable tool for evaluating outdoor thermal comfort. It is currently one of the most widely used indices and has been extensively applied by scholars [12][18]-[20].

(2) Existing studies on outdoor thermal environments have demonstrated a significant correlation between PET and thermal sensation votes, typically yielding a high coefficient of determination (R2) [21]-[24]. This indicates that PET is a reliable indicator for predicting outdoor thermal comfort.

The thermal comfort classification employs the following scale to describe human thermal comfort across different temperatures [25] (Table 1).

Table 1. Classification of Physiological Equivalent Temperature (PET) [25].

PET(℃)	Thermal Sensation	Physical Stress Level
＞41	Very hot	Extreme heat stress
35~41	Hot	Strong heat stress
29~35	Warm	Moderate heat stress
23~29	Slightly warm	Slight heat stress
18~23	Neutral (comfortable)	No thermal stress
13~18	Slightly cool	Slight cold stress
8~13	Cool	Moderate cold stress
4~8	Cold	Strong cold stress
≤4	Very cold	Extreme cold stress

2.2.2. Selection of Thermal Comfort Evaluation Indices

Spatial characteristics not only reflect the geometric morphology, plant configuration, and physical surface attributes of greenway spaces, but also encompass the influence of landscape elements on microclimate and thermal comfort. Drawing upon previous research concerning the environmental elements of the Qingshan Lake Greenway, this study categorizes its spatial environmental elements into three major groups: spatial elements, natural elements, and facility elements. Accordingly, specific indicators are selected based on these three categories as follows (Table 2).

Table 2. Spatial characteristic indicators of the Qingshan Lake Greenway.

Greenway Spatial Environment Elements	Indicator	Description	Source
Spatial Elements	Coverage Degree (CD)	The ratio of the vertical projection canopy cover area of trees >1.8 m high, or the accessible building space, to the total spatial area within the sample space.	Zhou et al. [26]
	Enclosure Degree (ED)	The ratio of the combined perimeter of small trees (<1.2 m high), shrubs, or structures within the sample space to the perimeter of the entire sample landscape space.	Zhou et al. [26]
	Sky View Factor (SVF)	Describes the openness of the sky, reflecting the degree of spatial enclosure.	Renzhi W et al. [27]
Natural Elements (Land, Vegetation, Water Body)	Terrain Visibility Rate (TVR)	Reflects the proportion of terrain occupied by landforms within the view domain, highlighting the salience of spatial skeleton and morphology.	Zhang et al. [29]
	Hard Visibility Rate (HVR)	Reflects the proportion of hard pavement within the view domain, emphasizing the performance of hardscape in the visual field.	Renzhi W et al. [27]
	Subsurface Permeability Rate (SPR)	The underlying surface properties are mainly recorded as two categories: impervious pavement (stone, concrete, brick) and permeable underlying surface (water body, green space, soil). The permeability is the ratio of the total permeable underlying surface area to the total land area available for use within the sample.	Zhang et al. [30]
	Green Space Ratio (GSR)	The ratio of the total green land area to the total land area within the land use scope, which is a basic indicator for measuring the greening and vegetation coverage of a region.	Zhang et al. [30]
	Green View Index (GVI)	Refers to the proportion of vegetation within the view domain, emphasizing the spatial effect of vegetation in the landscape on-site.	Renzhi W et al. [27], Li et al. [28]
	Blue View Index (BVI)	The proportion of water bodies in people's field of view, including lakes, streams, waterfalls, and other water features.	Li et al. [28]
Facility Elements	Facilities Visibility Rate (FVR)	Refers to the proportion of buildings or infrastructure within the view domain, emphasizing the spatial effect on the facade.	Luo et al. [31]

2.3. Data Collection and Processing

2.3.1. Microclimate Field Measurements

Hangzhou, situated in a subtropical monsoon climate zone, experiences generally high temperatures during summer. July and August represent the peak temperature months of the year, characterized by concentrated precipitation and high air humidity. Conducting measurements during this specific period can, therefore, more accurately capture the thermal environment characteristics of typical high-temperature summer days.

In this study, microclimate field measurements were conducted across the sample sites from August 15 to 20, 2025, employing a mobile measurement method. The specific measurement windows were set from 09:30 to 11:30 and 16:30 to 18:30. Each hour was designated as an independent observation

period, yielding a total of four periods. This schedule was selected because these periods fall within the operational hours of the Qingshan Lake Greenway and coincide with peak times for public recreational activities.

To dynamically monitor variations in air temperature, relative humidity, wind speed, solar radiation, and globe temperature, measurement instruments were mounted on electric scooters, which were driven at a constant speed. The sensors were positioned at a height of 1.5 m above the ground (Table 3). For each greenway section, climatic data across the sample sites were collected through two round trips completed within a half-hour timeframe. To minimize temporal errors, data collection across the five greenway sections was conducted simultaneously. These measurements were repeated over six consecutive days, and the average values were calculated for analysis. This methodological design comprehensively accounts for Hangzhou's climatic features, public travel patterns, and the specific usage characteristics of the Qingshan Lake Greenway.

Table 3. Technical specifications of the microclimate measurement instruments.

Instrument Model	Measured Parameter	Measurement Range	Resolution	Measurement Accuracy
Kestrel5500	Wind Speed (V)	0~60m/s	±3%	0.1m/s
	Air Temperature (Ta)	-29~70 ℃	0.5 ℃	0.1 ℃
	Relative Humidity (RH)	10%~90%	±2%	0.1%
TES 1333 (Taiwan)	Solar Radiation (G)	0~2000W/㎡	±0.1W/㎡	±10W/㎡
AZ8778 (AZ Instruments)	Black Globe Temperature (Tg)	0~80℃	0.1℃	±0.6℃

2.3.2. Quantification of Greenway Spatial Characteristics

In this study, an Insta360 X4 action camera was utilized to capture panoramic photos at each sample site. The shooting height was set at 1.60 m to simulate the normal eye-level field of view of an adult. These photos were used to obtain data for the Terrain Visibility Rate (TVR), Hard Visibility Rate (HVR), Green View Index (GVI), Blue View Index (BVI), and facility visibility rate. Simultaneously, a DJI Phantom 4 Pro unmanned aerial vehicle (UAV) was deployed to capture aerial images above each sample plot, acquiring data for the Coverage Degree (CD), Enclosure Degree (ED), Subsurface Permeability Rate (SPR), and Green Space Ratio (GSR).

Subsequently, a Pyramid Scene Parsing Network (PSPNet) semantic segmentation model [32], trained and optimized based on the ADE20K dataset [33], was applied to perform semantic segmentation on the panoramic photos. This process extracted various spatial composition elements to precisely quantify their spatial characteristics. Furthermore, the raw data were normalized to more intuitively reflect the relative magnitude relationships among the variables (Figure 2 and 3). For conciseness, the aforementioned indicators, along with the Sky View Factor (SVF), will be referred to by their respective abbreviations in the subsequent text.

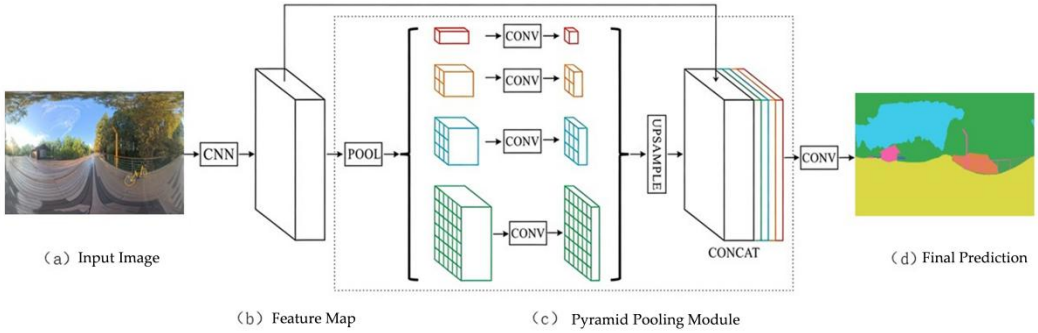

Figure 2. Working principle of the PSPNet model.

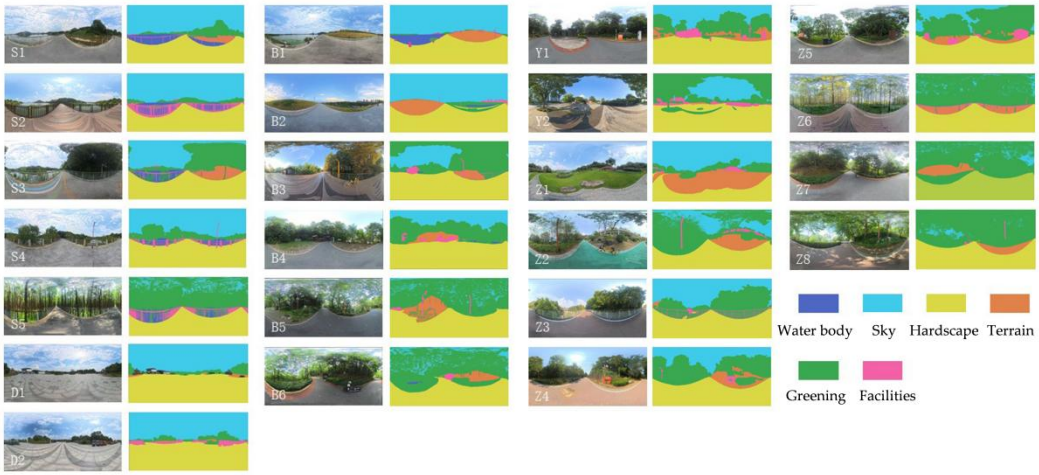

Figure 3. Semantic segmentation results of panoramic photos.

3. RESULTS

3.1. Analysis of Microclimate Field Measurement Data

Variations in air temperature (Figure 4): Temporally, the average air temperature across all spaces in the morning ranged from 31.8 to 37.3 °C, showing a gradual upward trend. The semi-shaded hardscape area exhibited the largest increase, while the fully shaded water area showed the smallest increase. In the afternoon, the average air temperature across all spaces ranged from 31.4 to 36.3 °C, displaying a gradual downward trend. The semi-shaded water area experienced the largest decrease, whereas the fully shaded water area had the smallest decrease. Spatially, the highest average air temperature occurred in the open water area, open waterfront area, and open lawn area at 37.2 ± 0.1 °C, which was approximately 0.2 °C lower than the control site during the same period. The lowest average air temperature was recorded in the fully shaded water area at 31.4 °C, which was 3.9 °C lower than the control site.

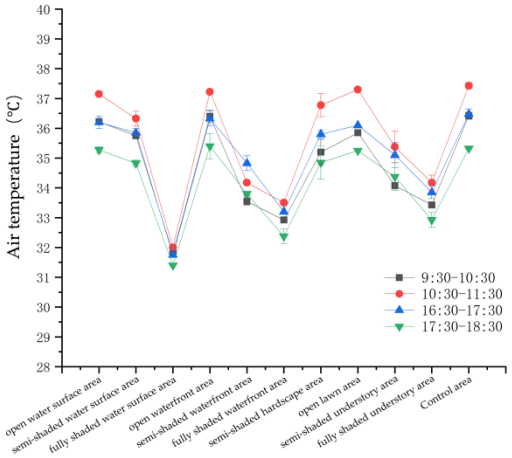

Figure 4. Variations in average air temperature.

Variations in relative humidity (Figure 5): Temporally, the average relative humidity across all spaces in the morning ranged from 57.33% to 72.55%. The fully shaded water area, open waterfront area, semi-shaded hardscape area, and fully shaded understory area experienced an increase in relative humidity, while other spaces showed a slight downward trend. In the afternoon, the relative humidity across all spaces ranged from 54.8% to 71.7%. The open water area, semi-shaded water area, fully shaded water area, and open lawn area showed an upward trend, whereas other spaces exhibited a slight decrease. Spatially, the fully shaded water area had the highest average relative humidity

(72.5%), which was 17.1% higher than the control site during the same period. The open water area recorded the lowest average relative humidity (54.8%), which was 0.7% higher than the control site.

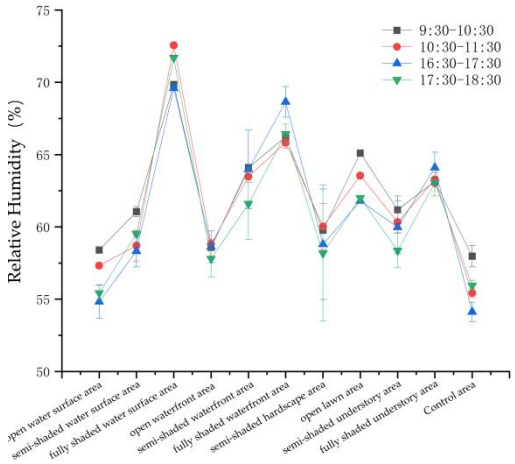

Figure 5. Variations in relative humidity.

Variations in wind speed (Figure 6): Temporally, the average wind speed across all spaces in the morning ranged from 0.1 to 0.55 m/s. The standard deviations of wind speed in the open waterfront area and semi-shaded hardscape area were relatively large, indicating noticeable fluctuations in these spaces. Wind speeds in other spaces fluctuated within a narrow range without obvious patterns. In the afternoon, wind speeds across all spaces ranged from 0.14 to 0.41 m/s, presenting a slight downward trend. Spatially, the open waterfront area recorded the highest average wind speed (0.55 m/s), which was 0.22 m/s higher than the control site during the same period. The fully shaded water area had the lowest average wind speed (0.1 m/s), which was 0.23 m/s lower than the control site.

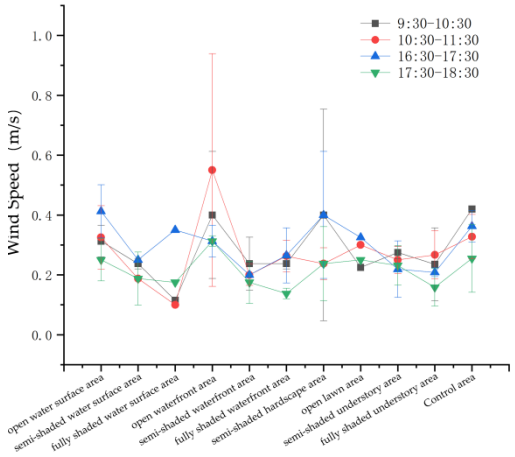

Figure 6. Variations in wind speed.

Variations in solar radiation (Figure 7): Temporally, the average solar radiation across all spaces in the morning ranged from 47.35 to 602.53 W/m², showing a gradual upward trend. The semi-shaded hardscape area and open lawn area experienced the largest increases, while the fully shaded water area and fully shaded understory area had the smallest increases. In the afternoon, solar radiation across all spaces ranged from 13.55 to 118.4 W/m², exhibiting a gradual downward trend. The open waterfront area showed the largest decrease, whereas the fully shaded water area, fully shaded waterfront area, and fully shaded understory area experienced the smallest decreases. Spatially, the open water area had the highest average solar radiation (602.53 W/m²), which was 114.3 W/m² higher than the control site during the same period. Fully shaded spaces recorded the lowest average solar radiation (20.2 ± 1.8 W/m²), which was 148.6 W/m² lower than the control site.

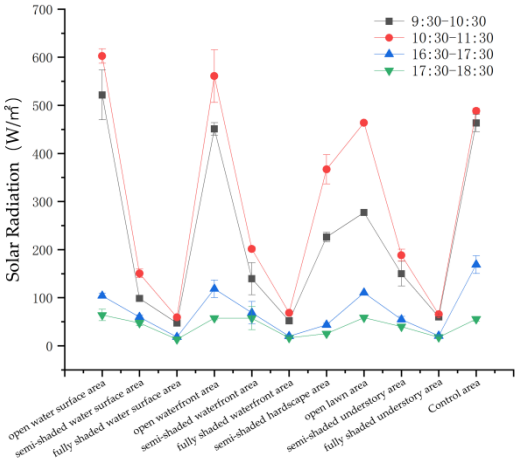

Figure 7. Variations in solar radiation.

Variations in globe temperature (Figure 8): Temporally, the average globe temperature across all spaces in the morning ranged from 33.85 to 43.1 °C, showing a gradual upward trend. The open lawn area exhibited the largest increase, while the fully shaded water area and fully shaded waterfront area showed the smallest increases. In the afternoon, the globe temperature across all spaces ranged from 33.1 to 40.7 °C, displaying a gradual downward trend. The decreases across all spaces were significantly smaller than that of the control site, with fully shaded spaces showing the smallest decrease. Spatially, the open water area and open lawn area recorded the highest average globe temperature (43.1 ± 0.1 °C), which was 0.4 °C lower than the control site during the same period. The fully shaded water area had the lowest average globe temperature (33.1 °C), which was 5 °C lower than the control site.

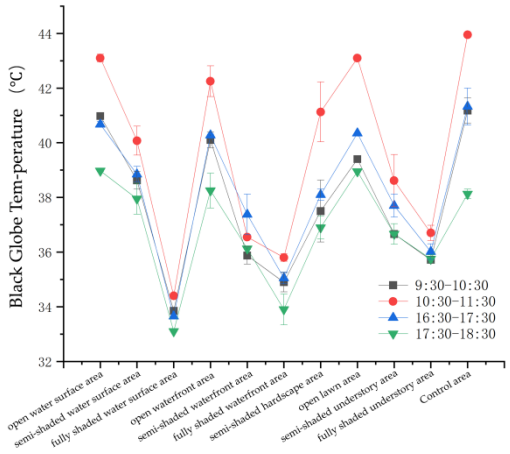

Figure 8. Variations in globe temperature.

3.2. Thermal Comfort Evaluation Based on Microclimatic Factors

As illustrated by the PET heatmap (Figure 9), thermal comfort levels varied across different periods and spatial types. The PET values for all sample sites ranged from 32.95 to 43.70 °C. PET values exhibited a significant negative correlation with thermal comfort; a lower PET value indicates a higher level of comfort. Therefore, as shown in the figure, among the four observation periods, the highest thermal comfort occurred in the evening (17:30–18:30), followed by the morning (09:30–10:30). Thermal comfort decreased in the late afternoon (16:30–17:30) and reached its lowest point at noon (10:30–11:30). Shaded spaces were more comfortable than open spaces. Under identical shading conditions, waterfront spaces were more comfortable than spaces further from the water.

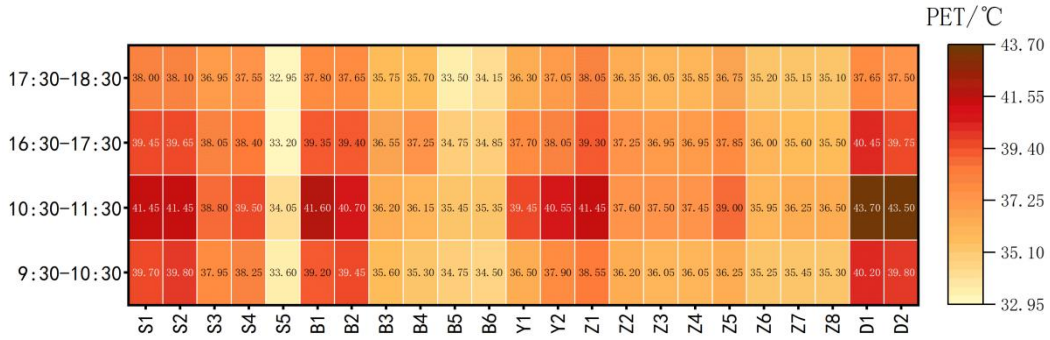

Figure 9. Heat map of average PET distribution

3.2.1. Thermal Comfort Evaluation Across Different Periods

Based on the thermal comfort classification scale, during the 09:30–10:30 period, the open water area, open waterfront area, and control site recorded the highest average PET values, with a thermal sensation categorized as "Hot." The fully shaded water area and fully shaded waterfront area were perceived as "Warm," while other spaces were felt as "Hot."

From 10:30 to 11:30, the open water area, open waterfront area, open lawn area, and control site were perceived as "Very hot," experiencing extreme heat stress, whereas most other spaces were felt as "Hot."

During the 16:30–17:30 period, the fully shaded water area and fully shaded waterfront area were perceived as "Warm," while other spaces felt "Hot."

From 17:30 to 18:30, the overall thermal sensations remained identical to those in the 16:30–17:30 period, but the PET values uniformly decreased by 1.5 ± 1.3 °C.

According to the PET heatmap, the ranking of comprehensive thermal comfort across the different periods was as follows: 17:30–18:30 > 09:30–10:30 > 16:30–17:30 > 10:30–11:30.

3.2.2. Thermal Comfort Evaluation Across Different Spatial Types

Among all greenway spatial types, the semi-shaded water area, semi-shaded waterfront area, semi-shaded hardscape area, semi-shaded understory area, and fully shaded understory area were all perceived as "Hot" across the four observation periods. Their average thermal comfort ranked as follows: fully shaded understory area > semi-shaded waterfront area > semi-shaded understory area > semi-shaded water area > semi-shaded hardscape area. The open water area, open waterfront area, open lawn area, and control site exhibited lower average thermal comfort, with most of these spaces perceived as "Very hot." Conversely, the fully shaded water area and fully shaded waterfront area demonstrated higher average thermal comfort, and were generally perceived as "Warm." As indicated by the PET heatmap, the comprehensive ranking of thermal comfort across different spatial types was: fully shaded water area > fully shaded waterfront area > fully shaded understory area > semi-shaded waterfront area > semi-shaded understory area > semi-shaded water area > semi-shaded hardscape area > open lawn area > open waterfront area > open water area > control site.

3.3. Quantification Results of Greenway Spatial Characteristics

Regarding landscape elements (Figure 10), fully shaded spaces exhibited the highest Green Space Ratio (GSR) and Green View Index (GVI). Sample site Z1 had a relatively high GSR but a low GVI because it is an open lawn space. Sites B3–B6 are waterfront spaces but recorded a low Blue View Index (BVI) (< 0.01). This is attributed to the influence of vegetation and topography; shrubs obscured part of the field of view, and the vertical distance between the road surface and the water surface was substantial. Water spaces had a low Terrain Visibility Rate (TVR) (< 0.05), whereas Z1 exhibited the highest TVR (0.244), indicating significant topographic undulations around this sample site. The Hard Visibility Rate (HVR) for most sample sites ranged between 0.3 and 0.4. Y1 and Y2

had a higher HVR, which may increase the spatial heat load and consequently negatively affect thermal comfort. The Subsurface Permeability Rate (SPR) also varied significantly among sample sites. Water spaces recorded the maximum values (> 0.70), while Y2, D1, and D2 had the minimum values (< 0.07). The landscape element indicators across different sample sites suggest that the degree of greening, the size of hardscape paving areas, surrounding topographic differences, and the types of underlying surfaces may all significantly influence thermal comfort.

Regarding spatial elements, the Coverage Degree (CD), Enclosure Degree (ED), and Sky View Factor (SVF) fluctuated considerably among the sample sites, indicating that the degree of spatial openness may impact thermal comfort. S5 recorded the highest CD and ED (> 0.95) along with a low SVF, suggesting that this space has the highest degree of shading, which likely helps improve thermal comfort. Conversely, S2, B1, and B2 had zero CD and ED but a high SVF, indicating that these spaces are highly open. While this extreme openness facilitates air circulation, these areas are simultaneously exposed to substantial solar radiation, thereby negatively affecting thermal comfort.

Regarding facility elements, the Facility Visibility Rate across all sample sites was less than 0.1, reflecting a small proportion of facilities within the greenway spaces. Y1 and Y2 had the highest Facility Visibility Rate, indicating a relative concentration of buildings and facilities in these spaces. The Facility Visibility Rate in other spaces fluctuated within a narrow range without significant differences.

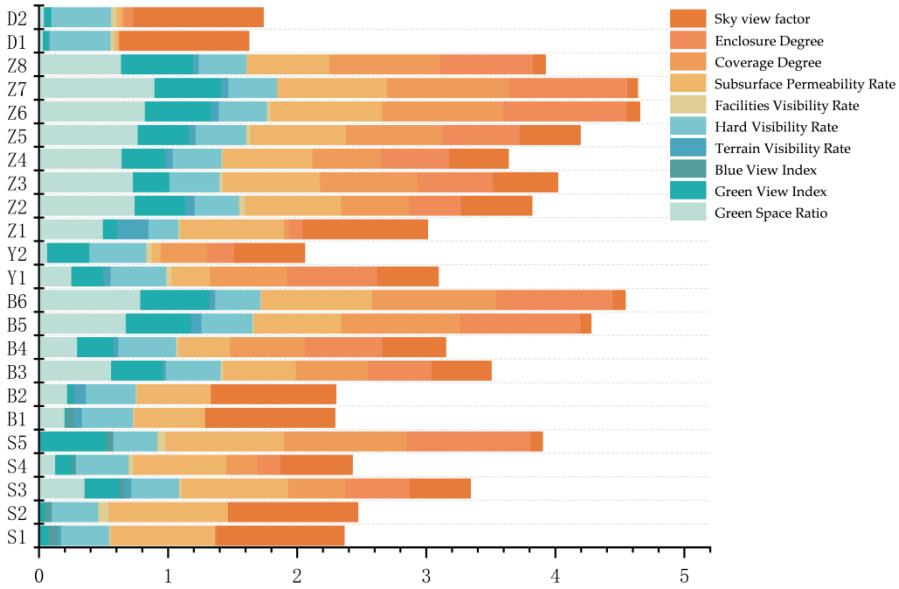

Figure 10. Quantification results of spatial characteristics in the Qingshan Lake Greenway.

3.4. Correlation Analysis Between Microclimatic Factors, PET, and Greenway Spatial Characteristics

To explore the correlations and impact degrees of different greenway spatial characteristics on thermal comfort, a Pearson correlation analysis was conducted between the ten spatial indicators, microclimatic factors, and PET. Indicators with $p > 0.05$ were excluded. The remaining indicators were then incorporated as variables into a stepwise regression analysis with the average PET.The correlation analysis revealed that the Facility Visibility Rate had no significant correlation with any microclimatic factors; therefore, this indicator was excluded. The correlations between the remaining indicators and the microclimatic factors are illustrated in the figure (Fig. 11).

According to the analysis results, Ta and Tg exhibited a strong negative correlation with GSR, GVI, SPR, CD, and ED, indicating that spaces with abundant greenery and high degrees of enclosure can effectively mitigate heat accumulation. RH showed a strong negative correlation with HVR and SVF,

suggesting that highly open spaces with larger hardscape paving areas are not conducive to increasing air humidity. V and G exhibited a strong negative correlation with GSR, GVI, CD, and ED, indicating that spaces with abundant greenery and high degrees of enclosure experience lower wind speeds and receive less solar radiation.

Furthermore, PET showed a strong negative correlation with GSR, GVI, SPR, CD, and ED, while exhibiting a strong positive correlation with SVF. This indicates that spaces with rich greenery, small hardscape paving areas, and high degrees of shading and enclosure can significantly enhance human thermal comfort.

Notably, BVI was positively correlated with PET, indicating that areas with larger water bodies paradoxically exhibited lower thermal comfort. This phenomenon may be attributed to two main reasons. First, near noon in summer, the water surface reflects a substantial amount of solar radiation, increasing the heat absorbed by the human body and thereby offsetting the cooling effect of the water body. Second, it may result from the synergistic effects of surrounding landscape elements. High-BVI areas typically have a lower GVI, which is a critical factor influencing microclimate and PET. The lack of green views might mask the potential cooling effect of the water body, leading to a negative impact of BVI on PET.

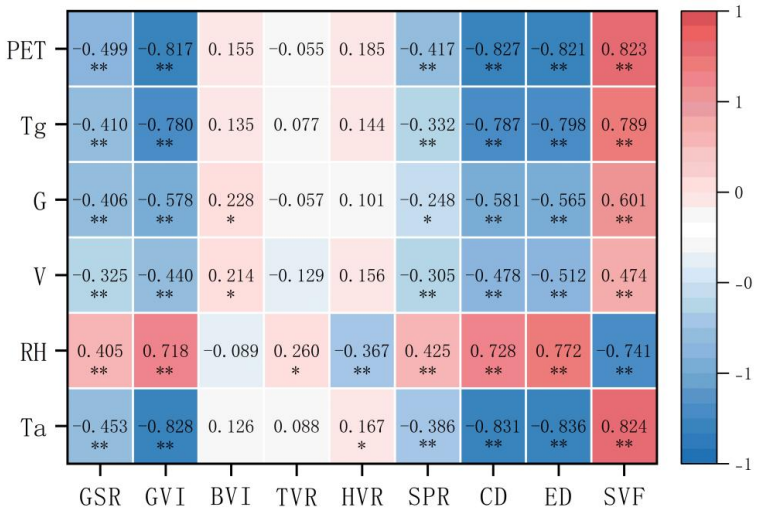

Figure 11. Correlation heatmap between microclimatic factors, PET, and greenway spatial characteristics. Note: ** Correlation is significant at the 0.01 level (2-tailed); * Correlation is significant at the 0.05 level (2-tailed).

3.5. Stepwise Regression Analysis of Microclimatic Factors, Average PET, and Significant Influencing Factors

To further investigate the relationships between the significantly correlated influencing factors, microclimate, and average PET, and to identify the indicators that exert a significant impact on the dependent variables, stepwise regression models were constructed. Specifically, the indicators that demonstrated significance in the correlation analysis were designated as independent variables, while the microclimatic factors and average PET were designated as dependent variables.

As indicated by the regression analysis (Table 4), the Green View Index (GVI) and Enclosure Degree (ED) exerted the greatest impact on air temperature (Ta), both demonstrating a significant negative effect. This indicates that increasing greenery and enhancing spatial enclosure play a positive role in reducing air temperature. The Hard Visibility Rate (HVR) had a significant negative effect on relative humidity (RH), whereas the Terrain Visibility Rate (TVR) and ED had a significant positive effect. This suggests that spaces with larger hardscape paving areas are detrimental to increasing relative humidity, while the presence of localized topography facilitates moisture retention. Furthermore, ED exerted a crucial influence on wind speed (V), and the Sky View Factor (SVF) significantly affected

solar radiation (G), indicating that the degree of spatial shading significantly impacts the thermal radiation within the greenway. The influencing indicators for globe temperature (Tg) were highly consistent with those for Ta.

Table 4. Stepwise regression aalysis of greenway spatial characteristic indicators, microclimatic factors, and average PET.

Dependent Variable	Model	B	SE	β	t	p	VIF	R2	Model Validation
Ta	(Constant)	36.876	0.208	-	177.022	0.000 ***	-	0.743	F=66.905 p < 0.001
	Enclosure Degree (ED)	-2.052	0.589	-0.492	-3.484	0.001 ***	7.064		
	Green Space Ratio (GSR)	1.109	0.342	0.239	3.245	0.002 ***	1.930		
	Green View Index (GVI)	-3.844	1.146	-0.486	-3.353	0.001 ***	7.443		
	Subsurface Permeability Rate (SPR)	-0.695	0.319	-0.129	-2.178	0.032 ***	1.241		
RH	(Constant)	65.258	2.544	-	25.650	0.000 ***	-	0.738	F=64.975 p < 0.001
	Enclosure Degree (ED)	11.569	0.865	1.012	13.375	0.000 ***	1.984		
	Hard Visibility Rate (HVR)	-20.950	5.871	-0.255	-3.568	0.001 ***	1.777		
	Green Space Ratio (GSR)	-5.858	1.133	-0.462	-5.172	0.000 ***	2.763		
	Terrain Visibility Rate (TVR)	20.102	7.187	0.237	2.797	0.006 ***	2.485		
V	(Constant)	0.343	0.017	-	20.206	0.000 ***	-	0.254	F=32.056 p < 0.001
	Enclosure Degree (ED)	-0.169	0.030	-0.512	-5.662	0.000 ***	1.000		
G	(Constant)	-3.474	25.656	-	-0.135	0.893	-	0.354	F=50.787 p < 0.001
	Sky View Factor (SVF)	287.731	40.375	0.601	7.127	0.000 ***	1.000		
Tg	(Constant)	40.674	0.202	-	201.288	0.000 ***	-	0.665	F=61.084 p < 0.001
	Enclosure Degree (ED)	-2.790	0.794	-0.565	-3.516	0.001 ***	7.008		
	Green Space Ratio(GSR)	1.208	0.447	0.221	2.701	0.008 ***	1.809		
	Green View Index(GVI)	-3.781	1.551	-0.404	-2.438	0.017 ***	7.441		
PET	(Constant)	40.261	0.329	-	122.512	0.000 ***	-	0.701	F=72.183 p < 0.001
	Coverage Degree (CD)	-5.390	0.483	-0.877	-11.169	0.000 ***	1.879		
	Subsurface Permeability Rate (SPR)	-1.331	0.527	-0.161	-2.526	0.013 ***	1.234		
	Green Space Ratio (GSR)	1.157	0.572	0.163	2.024	0.046 ***	1.967		

The coefficient direction and significance of ED varied across different models. This reveals that, under the combined interaction of multiple microclimatic factors, enhancing spatial enclosure is beneficial for lowering air temperature, increasing humidity, and mitigating thermal radiation, but it is disadvantageous for enhancing wind speed. Interestingly, the impact of the Green Space Ratio (GSR) on Ta, RH, Tg, and PET contradicted the results of the initial correlation analysis. This discrepancy may be attributed to the comprehensive interaction of other environmental factors within specific contexts, demonstrating the inherent complexity of how greenway spatial characteristics affect microclimate and thermal comfort.

Overall, in the stepwise regression analysis accounting for the comprehensive effects of multiple variables, GSR, GVI, and ED emerged as the spatial characteristic indicators with the greatest impact on microclimatic factors. Meanwhile, average PET was primarily influenced by GSR, the Subsurface Permeability Rate (SPR), and the Coverage Degree (CD).

The regression models linking microclimatic factors and PET to greenway spatial characteristics all exhibited strong statistical significance (Table 5), indicating a good overall model fit ($p < 0.001$). Notably, the regression models for wind speed (V) and solar radiation (G) retained only a single independent variable. This indicates that wind speed is primarily associated with the degree of spatial enclosure, whereas solar radiation is predominantly determined by the degree of spatial shading.

Regarding explanatory power (R2), the regression models for Ta, RH, Tg, and PET demonstrated relatively high values, whereas the models for V and G yielded slightly lower values. This underscores that greenway spatial characteristics exert a more pronounced and significant influence on air temperature, relative humidity, globe temperature, and human thermal comfort (PET).

Table 5. Stepwise regression models linking greenway spatial characteristics to microclimatic factors and average PET.

Dependent Variable	Regression Model	R2
Ta	Y = 36.876 + 1.109 * GSR - 3.844 * GVI - 0.695 * SPR - 2.052 * ED ($p < 0.001$)	0.743
RH	Y = 65.258 - 5.858 * GSR - 20.950 * HVR + 20.102 * TVR + 11.569 * ED ($p < 0.001$)	0.738
V	Y = 0.343 - 0.169 * ED ($p < 0.001$)	0.254
G	y=-3. 474+287.731* SVF ($p < 0.001$)	0.354
Tg	Y = 40.674 + 1.208 * GSR - 3.781 * GVI - 2.790 * ED ($p < 0.001$)	0.665
PET	Y = 40.261 + 1.157 * GSR - 1.331 * SPR - 5.390 * CD ($p < 0.001$)	0.701

4. DISCUSSION

Studies have demonstrated that greenway spaces play a positive role in improving the thermal environment and human thermal comfort. According to the field measurement results, the air temperature, solar radiation, and globe temperature within the greenway spaces were lower than those in the control site, while the relative humidity was higher. This enables people to achieve a more comfortable recreational experience within the greenway. This finding is highly consistent with several previous studies [34],[35].

Previous studies have indicated a positive correlation between water body area, relative humidity, and PET [36],[37]. In this study, the thermal comfort of fully shaded spaces near the water was

significantly higher than that of fully shaded spaces further from the water. However, the average PET of open and semi-shaded spaces near the water showed no significant difference compared to their counterparts further from the water. On the one hand, this may be due to the severe lack of shading in the near-water sample sites, leading to higher solar radiation and consequently elevating the PET. Conversely, spaces further from the water possessed a higher Subsurface Permeability Rate (SPR), which stores less heat and, to some extent, improves the surrounding thermal environment. On the other hand, the low albedo of water bodies means that they absorb the vast majority of solar radiation, causing the water surface itself to heat up and release substantial long-wave thermal radiation into the adjacent air layer and surrounding environment. Under calm or light wind conditions, this heating effect may dominate in the near-water areas, resulting in an elevated PET.

Furthermore, in this study, the Facility Visibility Rate showed no significant correlation with microclimatic factors and PET. This may be because the facilities within the greenway predominantly consist of small-scale service amenities, such as streetlights and trash bins. Although service buildings occasionally appear, their small footprint and low height prevent them from exerting a significant impact. Specifically, small-scale buildings cannot fully block solar radiation to lower the PET. Additionally, the construction materials of the buildings in the greenway are mostly wooden, which absorb less heat compared to other building materials. These two reasons explain why the Facility Visibility Rate in the greenway exhibited no correlation with microclimatic factors and PET.

This study conducted field measurements over six consecutive days in mid-August, effectively capturing the typical thermal environmental characteristics of summer in the subtropical monsoon climate of the hot-summer and cold-winter region. By applying multi-day averaging, random errors were further reduced, thereby enhancing the representativeness and stability of the results.Regarding the observation periods (9:30–11:30 a.m. and 4:30–6:30 p.m.), the study closely aligns with the summer climatic patterns of Hangzhou as well as the peak recreational and travel periods of the public along the Qingshan Lake Greenway.Although this phase of the study provides an accurate characterization of microclimatic patterns within a specific spatiotemporal context, the scope of observations is limited by the monitoring period and site conditions. As a result, other seasons and non-peak periods were not covered, which imposes certain limitations on the broader spatial and seasonal generalizability of the findings.

5. CONCLUSIONS

This study collected microclimate data across four periods and 10 different spatial types in the Qingshan Lake Greenway during summer. Based on UAV imagery and field surveys, semantic segmentation was employed to extract and quantify greenway spatial characteristics. Stepwise regression analysis was then applied to reveal the relationships between various spatial indicators, microclimate, and thermal comfort. The main conclusions are as follows:

(1) Temporally, the thermal comfort of the same spatial type varied across different periods. During the morning periods, the PET gradually increased; open spaces were predominantly perceived as "Very hot" from 10:30 to 11:30, while the remaining spaces were mostly perceived as "Hot." During the afternoon periods, the PET gradually decreased; open and semi-shaded spaces were mostly perceived as "Hot," whereas fully shaded spaces were generally perceived as "Warm." Spatially, the thermal comfort of different spaces varied within the same period. At an identical distance from the water surface, spaces with a higher degree of shading were more comfortable. Under identical shading conditions, spaces closer to the water were more comfortable.

(2) In the Qingshan Lake Greenway during summer, vegetation, water bodies, underlying surfaces, and the degree of spatial enclosure and coverage all impacted thermal comfort. Notably, the amount of greenery, the permeability of the underlying surface, and the degree of spatial shading were the

most critical factors influencing human thermal comfort. Additionally, the Facility Visibility Rate exhibited no significant correlation with microclimate and thermal comfort.

(3) The relationships between spatial characteristic indicators, microclimatic factors, and PET are not simply linear. The constructed stepwise regression models, applicable to summers in climate zones characterized by hot summers and cold winters, successfully screened out the indicators with significant impacts on the dependent variables. These models intuitively explain the influence intensity and underlying correlation mechanisms of summer greenway spatial characteristics on microclimatic factors and PET.

Based on the above conclusions, corresponding optimization strategies for greenway spaces are proposed: Firstly, appropriately increase the green coverage rate and enrich the vegetation hierarchy. It is recommended to select arbor trees with large canopies, tall trunks, and moderate leaf areas to balance shading and ventilation while enhancing spatial coverage. Secondly, replace existing paving with permeable pavements (e.g., permeable bricks and pervious concrete), which can effectively improve the thermal environment and enhance the water cycle. Thirdly, improve the matching degree between landscape and function according to usage periods. Mornings and late afternoons are high-frequency periods for moderate-to-high intensity activities in the greenway; therefore, arbor trees with large canopies can be utilized to provide low-angle shading and create a comfortable activity environment. Concurrently, combining arbor trees with recreational facilities can block high-angle solar radiation, creating comfortable shaded spaces for low-intensity activities at noon.

Finally, for open near-water spaces with lower summer comfort, aquatic plants and water-tolerant tall trees can be planted to expand the shaded area and enhance landscape aesthetics. For open spaces further from the water, adding artificial facilities such as pavilions can effectively reduce site temperatures [38]. Simultaneously, installing mist spraying systems can efficiently achieve cooling and humidification [39],[40], thereby creating a healthy and comfortable greenway environment for the public.

CONFLICTS OF INTEREST

The authors declare no conflicts of interest.

ACKNOWLEDGEMENTS

This research received no external funding.

REFERENCES

[1] United Nations Human Settlements. Envisaging the Future of Cities: World Cities Report 2022 [R]. Nairobi: United Nations Human Settlements Programme,2022[2023-10-05]. https://unhabitat.org/wcr/2022.

[2] CHEVANCE G, MINOR K, VIELMA C, et al. A systematic review of ambient heat and sleep in a warming climate[J]. Sleep Medicine Reviews, 2024, 75:101915. DOI:10.1016/j.smrv.2024.101915.

[3] LIU Y, ZHANG W, LIU W, et al. Exploring the seasonal effects of urban morphology on land surface temperature in urban functional zones[J]. Sustainable Cities and Society, 2024, 103:105268.

[4] Liu Y ,Yuan Z ,Luo J , et al.The impact of 3D urban landscapes on multidimensional human experience: An interpretable machine learning approach[J].Building and Environment,2026,293114320-114320.DOI:10.1016/J.BUILDENV.2026.114320.

[5] Ding W W, Hu Y P, Dou P P. Research on the correlation between urban form and urban microclimate[J]. Architectural Journal, 2012(7): 16-21.

[6] Xue S H, Liu M, Wang K, et al. Analysis of autumn thermal comfort characteristics and influencing factors of the elderly in urban parks in cold regions[J]. Science Technology and Engineering, 2024, 24(1): 336-343.

[7] Luo M Y. Analysis of microclimate optimization strategies in newly built residential areas of Changsha[J]. Urbanism and Architecture, 2023, 20(4): 81-83. https://doi.org/10.19892/j.cnki.csjz.2023.04.21.

[8] Zheng G R, Wang S T, Lin X Y, et al. Analysis on optimal design of campus green space based on microclimate: a case study of Fujian Agriculture and Forestry University[J]. Urbanism and Architecture, 2024, 21(14): 112-114. https://doi.org/10.19892/j.cnki.csjz.2024.14.26.

[9] Liang C. Study on summer microclimate effect of urban waterfront greenway in subtropical region[D]. South China University of Technology, 2020. https://doi.org/10.27151/d.cnki.ghnlu.2020.001060.

[10] Li J N. Evaluation and optimization of thermal comfort of urban greenway[D]. Beijing University of Civil Engineering and Architecture, 2022. https://doi.org/10.26943/d.cnki.gbjzc.2022.000086.

[11] Dong L. Beijing Three Mountains and Five Gardens Greenway: study on usage characteristics and satisfaction of historical and cultural greenway[J]. Beijing Planning Review, 2020(5): 115-118.

[12] Huang R X, Yu K Y, Liu J. Analysis of factors influencing park thermal comfort under extreme high temperature: a case study of Fuzhou Chating Park[J]. Chinese Landscape Architecture, 2024, 40(10): 99-105. https://doi.org/10.19775/j.cla.2024.10.0099.

[13] Xu J ,Wei Q ,Huang X , et al.Evaluation of human thermal comfort near urban waterbody during summer[J].Building and Environment,2009,45(4):1072-1080.DOI:10.1016/j.buildenv.2009.10.025.

[14] Sun C Y .A street thermal environment study in summer by the mobile transect technique[J].Theoretical and Applied Climatology, 2011, 106(3-4):433-442.DOI:10.1007/s00704-011-0444-6.

[15] Effect of land cover on air temperatures involved in the development of an intra-urban heat island[J].Climate Research,2009,39(1):61-73.

[16] Chen X, Sun R H, Li J Y. Research progress and prospect of urban human thermal comfort evaluation[J]. Environmental Ecology, 2023, 5(9): 28-36.

[17] Hppe P R .The physiological equivalent temperature - A universal index for the biometeorological assessment of the thermal environment[J].International Journal of Biometeorology, 1999, 43(2):71-75.DOI:10.1007/s004840050118.

[18] Yi M ,Lili X .Research on Seasonal Thermal Neutral Temperature in West Lake Scenic Area of Hangzhou, China[J].International Journal of Environmental Research and Public Health,2022,19(22):14677-14677.DOI:10.3390/IJERPH192214677.

[19] Labdaoui K , Mazouz S , Moeinaddini M ,et al.The Street Walkability and Thermal Comfort Index (SWTCI): A new assessment tool combining street design measurements and thermal comfort[J].Science of The Total Environment, 2021:148663.DOI:10.1016/j.scitotenv.2021.148663.

[20] Li, Y., Shu, L., & Huang, L. Thermal comfort of communities with different green coverage in Minjiang Park, Fuzhou City. Sichuan Forestry Science and Technology, 2023, 44(01), 72-76.

[21] Elnabawi M H , Hamza N .Outdoor Thermal Comfort: Coupling Microclimatic Parameters with Subjective Thermal Assessment to Design Urban Performative Spaces[J].Buildings, 2020, 10(12):238.DOI:10.3390/buildings10120238.

[22] Lin D , Li T , Chen Z ,et al.Effects of interactions between thermal and acoustic environments on subjective comfort evaluations in outdoor public spaces[J].Journal of Asian Architecture and Building Engineering, 2025, 24(1):367-382.DOI:10.1080/13467581.2023.2292069.

[23] Ma, Z. R., Liu, J., & Chen, T. Evaluation and research on human thermal comfort and physiological response in residential streets of high-density urban areas. Landscape Design,2025, 23(3), 18–23.

[24] Zuo J, Zhang H L, Yu M S, Wei Q S, Wang Z N, Fan J H. Multi-dimensional evaluation of outdoor thermal comfort in built environments of high-density old communities in humid and hot areas: a case study of Shentian Community in Xiamen. Acta Ecologica Sinica, 2025, 45(12): 5674-5689.

[25] Cheung K P ,Jim C .Comparing the cooling effects of a tree and a concrete shelter using PET and UTCI[J].Building and Environment,2018,13049-61.DOI:10.1016/j.buildenv.2017.12.013.

[26] Zhou X, Jin S J, Che S Q. Research on the relationship between spatial characteristics and privacy of urban park plant communities: a case study of Hangzhou[J]. Chinese Landscape Architecture, 2012, 28(5): 99-103.

[27] Renzhi W ,Xiaoshan F ,Robert B , et al.Establishing a link between complex courtyard spaces and thermal comfort: A major advancement in evidence-based design[J].Building and Environment,2023,245DOI:10.1016/J.BUILDENV.2023.110852.

[28] Li J Y, Lin Y F, Dong J W, et al. Research on beauty evaluation of urban waterfront green space based on semantic segmentation: a case study of Fuzhou West Lake Park and Zuohai Park[J]. Chinese Landscape Architecture, 2022, 38(10): 92-97. https://doi.org/10.19775/j.cla.2022.10.0092.

[29] Zhang X H, Cheng Z Q, Zhang N. From viewpoint to space: a quantitative analysis method of landscape spatial visual characteristics based on point cloud[J]. Landscape Architecture, 2024, 31(7): 115-121.

[30] Zhang Q, Chen T, Zang X Y. Analysis of influencing factors on summer microclimate in external spaces of old university campuses: a case study of Tianjin[J]. Building Energy Conservation, 2020, 48(1): 85-92.

[31] Luo J J, Lei Z X, Kong X Y, et al. Research on visual perception of urban river landscape based on computer vision technology[J]. Chinese Landscape Architecture, 2025, 41(2): 78-85. https://doi.org/10.19775/j.cla.2025.02.0078.

[32] Zhao H , Shi J , Qi X ,et al.[IEEE 2017 IEEE Conference on Computer Vision and Pattern Recognition (CVPR) - Honolulu, HI (2017.7.21-2017.7.26)] 2017 IEEE Conference on Computer Vision and Pattern Recognition (CVPR) - Pyramid Scene Parsing Network[C]//2017:6230-6239.DOI:10.1109/cvpr.2017.660.

[33] Zhou B ,Zhao H ,Puig X , et al.Semantic Understanding of Scenes Through the ADE20K Dataset[J].International Journal of Computer Vision,2019,127(3):302-321.DOI:10.1007/s11263-018-1140-0.

[34] Deng Z Q, Chao J, Shen Q, et al. Discussion on the improvement effect of greenway on block microclimate based on ideal unit[J]. Building Energy Conservation, 2020, 48(9): 90-96.

[35] Wang Q, Zhong B T. Research on the impact of greenways on microclimate in high-density cities[J]. Community Design, 2019(1): 25-32.

[36] Xiong Y, Zhang F, Li L, et al. Numerical simulation of thermal environment in Changsha Taiping Street historical and cultural block based on green space microclimate[J]. Tropical Geography, 2023, 43(2): 330-342. https://doi.org/10.13284/j.cnki.rddl.003634.

[37] Xuefan Z ,Shuai Z ,Yingfei L, et al.Impact of urban morphology on the microclimatic regulation of water bodies on waterfront in summer: A case study of Wuhan[J].Building and Environment,2022,226DOI:10.1016/J.BUILDENV.2022.109720.

[38] Jin, W.; Fukuda, H. Strategies for Enhancing the Thermal Environment of Street Spaces in Ancient Canal Towns Based on the Design of Water-Friendly Spatial Diversity. Sustainability 2025, 17, 3112. https://doi.org/10.3390/su17073112

[39] Su M , Hong B , Su X ,et al.How the nozzle density and height of mist spraying affect pedestrian outdoor thermal comfort: A field study[J].Building and environment, 2022(May):215.DOI:10.1016/j.buildenv.2022.108968.

[40] Deng, Y., Jiang, W. G., Ling, Z. Y., et al. Thermal environment and summer heat mitigation potential assessment of urban wetland parks in Chengdu. Scientia Geographica Sinica, 2025, 45(2), 403–414. https://doi.org/10.13249/j.cnki.sgs.20240391